



International Specialty Conference on Cold-Formed Steel Structures

(2008) - 19th International Specialty Conference on Cold-Formed Steel Structures

Oct 14th, 12:00 AM

Simplified Methods for Predicting Elastic Buckling of Cold-formed Steel Structural Members with Holes

Christopher D. Moen

Follow this and additional works at: <https://scholarsmine.mst.edu/isccss>



Part of the [Structural Engineering Commons](#)

Recommended Citation

Moen, Christopher D., "Simplified Methods for Predicting Elastic Buckling of Cold-formed Steel Structural Members with Holes" (2008). *International Specialty Conference on Cold-Formed Steel Structures*. 5. <https://scholarsmine.mst.edu/isccss/19iccfss/19iccfss-session1/5>

This Article - Conference proceedings is brought to you for free and open access by Scholars' Mine. It has been accepted for inclusion in International Specialty Conference on Cold-Formed Steel Structures by an authorized administrator of Scholars' Mine. This work is protected by U. S. Copyright Law. Unauthorized use including reproduction for redistribution requires the permission of the copyright holder. For more information, please contact scholarsmine@mst.edu.

Simplified Methods for Predicting Elastic Buckling of Cold-Formed Steel Structural Members with Holes

Cristopher D. Moen¹, B.W. Schafer²

Abstract

Simplified methods for approximating the local, distortional, and global critical elastic buckling loads of cold-formed steel columns and beams with holes are developed and summarized. These methods are central to the extension of the Direct Strength Method (DSM) to members with holes, as DSM employs elastic buckling properties to predict ultimate strength. The simplified methods are developed as a convenient alternative to shell finite element eigenbuckling analysis, which requires commercial software not always accessible to the engineering community. A variety of simplified methods are pursued including (a) hand methods founded primarily on classical plate stability approximations and (b) empirical extensions to the semi-analytical finite strip method (i.e., modifying and using the freely available, open source software, CUFSM). The proposed methods are verified with shell finite element eigenbuckling studies. The developed simplified methods are intended to be general enough to accommodate the range of hole shapes, locations, and spacings common in industry, while at the same time also defining regimes where explicit use of shell finite element analyses are still needed for adequate accuracy.

Introduction

The forthcoming implementation of the Direct Strength Method (AISI-S100 2007; Schafer 2008) for cold-formed steel structural members with holes may be aided greatly by approximate methods for predicting elastic buckling behavior. Early research evaluated the influence of a single hole on the elastic buckling of

¹ Graduate Research Asst, Johns Hopkins University, Baltimore, MD, 21218, USA. (moen@jhu.edu)

² Associate Professor, Johns Hopkins University, Baltimore, MD, 21218, USA. (schafer@jhu.edu)

a thin square plate (Kumai 1952; Schlack Jr. 1964; Yoshiki and Fujita 1967). Holes were observed to reduce bending stiffness and concentrate the axial stress in the plate strips adjacent to the hole. This research led to a useful approximation of elastic buckling stress for plates with holes, based on assuming the strips adjacent to the hole act as unstiffened elements in compression (Kawai and Ohtsubo 1968). This approximation laid the groundwork for the development of the Specification's "unstiffened strip" approach, where elastic buckling of the plate strips are used to predict ultimate strength with the effective width method (Vann 1971; Yu and Davis 1973; Miller and Peköz 1994).

More recent thin shell finite element research on the elastic buckling of rectangular plates with multiple holes has demonstrated that the presence of holes can either increase or decrease the critical elastic buckling stress and change the length and quantity of the buckled half-waves, depending upon the quantity of hole material removed relative to the size of the plate (Brown and Yettram 2000; El-Sawy and Nazmy 2001; Moen and Schafer 2006). Research on an approximate method for calculating the critical elastic buckling loads of cold-formed steel columns with holes using the semi-analytical finite strip method has shown promise (Tovar and Sposito 2005). Progress on predicting the local, distortional, and global buckling of cold-formed steel rack posts with arrays of small holes has also been achieved (Kesti 2000; Sarawit 2003). The work presented here focuses on holes common in cold-formed steel framing, where multiple holes may exist along the length, but typically only a single hole exists in any one element (i.e., web or flange).

To facilitate the use of DSM for members with holes, approximate (and conservative) methods for calculating the elastic buckling of cold-formed steel members with holes are presented in this paper. The simplified approaches can be used in lieu of a full finite element eigenbuckling analysis. Elastic buckling approximations based on classical plate stability equations are presented for stiffened and unstiffened elements with holes. Finite strip approximations for local and distortional buckling of full cold-formed steel members with holes are introduced, and modifications to the classical column and beam stability equations are proposed for global buckling of members with holes. The simplified methods are intended to be general enough to accommodate the range of hole shapes, sizes, and spacings common in industry.

Elastic buckling of elements with holes

Approximate elastic buckling prediction methods are presented here for two common element types in a thin-walled cross-section, stiffened elements (e.g.,

flange or web of a C-section) and unstiffened elements (e.g., flange lip of a C-section). In design, a stiffened element is approximated as a simply-supported plate and an unstiffened element is treated as a plate simply-supported on three sides and free on the fourth edge parallel to the application of load. Element and hole dimension notation for the prediction methods are summarized in Figure 1. The strips of plate between a hole and the plate edges are referred to as unstiffened strip “A” and unstiffened strip “B”. For stiffened elements in bending, the neutral axis location Y is measured from the compressed edge of the plate. Finally, δ_{hole} is the transverse offset distance of a hole measured from the centerline of the plate.

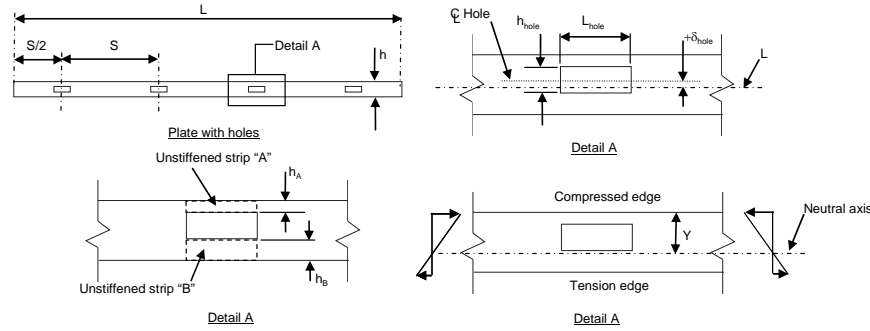


Figure 1 Element and hole dimension definitions

The viability of the element prediction methods has been verified within the following geometric limits (Moen 2008):

$$\frac{L_{hole}}{h_A} \leq 10, \frac{L_{hole}}{h_B} \leq 10, \frac{h_{hole}}{h} \leq 0.50, \frac{S}{L_{hole}} \geq 2, \frac{S}{h} \geq 1.5. \quad (1)$$

Stiffened element in uniaxial compression

This approximate method predicts the critical elastic buckling stress of stiffened elements with holes under uniaxial compression considering two potential elastic buckling states: buckling of the plate without influence from the hole(s), or buckling of the unstiffened strips adjacent to a hole, as shown in Figure 2.

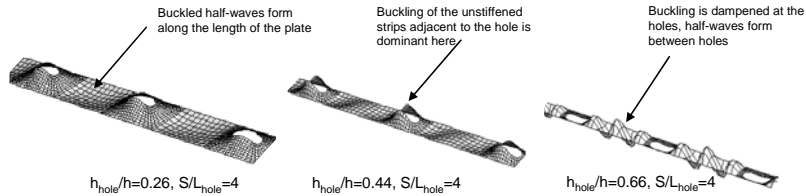


Figure 2 Buckled mode shapes for a stiffened element with holes

The elastic buckling stress of a stiffened element with holes is approximated as

$$f_{crf} = \min[f_{cr}, f_{crh}] \quad (2)$$

The critical elastic buckling stress for plate buckling (without hole influence) is

$$f_{cr} = k \frac{\pi^2 E}{12(1-\nu^2)} \left(\frac{t}{h}\right)^2, \quad (3)$$

where k is commonly taken equal to 4 when considering long rectangular plates ($L/h > 4$). When elastic buckling of the stiffened element is governed by the buckling of an unstiffened strip adjacent to the hole, the critical elastic buckling stress of the governing unstiffened strip is:

$$f_{crh,net} = \min[f_{crA}, f_{crB}] \quad (4)$$

$$f_{cri} = k_i \frac{\pi^2 E}{12(1-\nu^2)} \left(\frac{t}{h_i}\right)^2 \text{ and } i = A \text{ or } B \quad (5)$$

The plate buckling coefficient k_i for unstiffened strips A and B are approximated by (Yu and Schafer 2007):

$$\text{for } L_{hole}/h_i \geq 1, \quad k_i = 0.425 + \frac{0.2}{(L_{hole}/h_i)^{0.95} - 0.6}, \quad (6)$$

$$\text{for } L_{hole}/h_i < 1, \quad k_i = 0.925, \text{ and } i = A \text{ or } B. \quad (7)$$

Eq. (6) accounts for the length of the unstiffened strip, as hole length shortens relative to the unstiffened strip width, k_i increases. This is an improvement over AISI-S100 which conservatively assumes the lowerbound $k=0.425$ regardless of hole length. When L_{hole}/h_i is less than 1, k may be conservatively assumed equal to 0.925 via Eq. (7) or calculated directly by solving the classical stability equations for an unstiffened element (Timoshenko 1961).

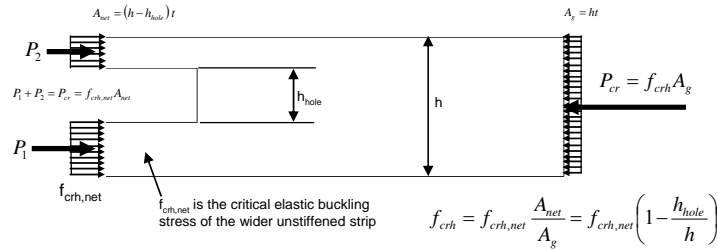


Figure 3 Unstiffened strip elastic buckling stress conversion from the net to the gross section

To compare the buckling stress from the unstiffened strip ($f_{crh,net}$) to that of the entire plate (f_{cr}) equilibrium between the net and gross section must be considered, as shown in Figure 3 and provided in the following:

$$f_{crh} = f_{crh,net} \left(1 - \frac{h_{hole}}{h}\right). \quad (8)$$

Stiffened element in bending

Similar to the stiffened element in uniaxial compression, a stiffened element in bending must consider buckling of the unstiffened strips on either side of the hole, or buckling of the stiffened element independent of the holes, as illustrated in Figure 4. Either buckling of the unstiffened strip between the hole and the compressed edge of the plate (unstiffened strip “A”) or the tension edge of the plate (unstiffened strip “B”) may occur depending upon the transverse location of the hole in the plate, the width of the hole (h_{hole}) relative to the depth of the plate (h), and the location of the plate neutral axis (Y). If the hole is completely contained within the tension region of the plate then the hole has a minimal influence on elastic buckling.



Figure 4 Buckled mode shapes for a stiffened element in bending

The critical elastic buckling stress of a stiffened element with holes in bending is approximated as:

$$f_{cr} = \min[f_{cr}, f_{crh}] \quad (9)$$

The critical elastic buckling stress for a stiffened element in bending (without the influence of holes), f_{cr} , may be determined with Eq. (3), where the buckling coefficient k is calculated with AISI-S100-07 Eq. B2.3-2 (AISI-S100 2007):

$$k = 4 + 2(1 + \psi)^3 + 2(1 + \psi) \quad (10)$$

and ψ is the absolute value of the ratio of tensile stress to compressive stress applied to the stiffened element, i.e.:

$$\psi = |f_2 / f_1| = (h - Y) / Y \quad (11)$$

When elastic buckling of the stiffened element is governed by the buckling of an unstiffened strip adjacent to a hole, the critical elastic buckling stress is:

$$f_{crh,net} = \min[f_{crA}, f_{crB}] \quad (12)$$

Consideration of unstiffened strip “A” is required only if $h_A < Y$, i.e., at least a portion of the hole must lie in the compression region of the stiffened element. If that condition is met the elastic buckling stress for strip “A” is:

$$f_{crA} = k_A \frac{\pi^2 E}{12(1 - \nu^2)} \left(\frac{t}{h_A} \right)^2 \quad (13)$$

The plate buckling coefficient for the unstiffened strip “A” is approximated as

$$k_A = \frac{0.578}{\psi_A + 0.34} + \frac{2.70 - 1.76\psi_A}{0.024\psi_A + 0.035 + (L_{hole}/h_A)^2}, \text{ and } \psi_A = \frac{Y - h_A}{Y} \quad (14)$$

Eq. (14) is a modification of AISI-S100-07 Eq. B3.3-2 (AISI-S100 2007). This expression accounts for the gradient of the compressive stress distribution and the aspect ratio of the unstiffened strip (Moen 2008).

Consideration of unstiffened strip “B” is required only if $h_A + h_{hole} < Y$, i.e., only when the entire hole lies within the compressed region of the plate. For this case the buckling stress of the unstiffened strip, converted to a stress at the compressed edge is found as:

$$f_{crB} = k_B \frac{\pi^2 E}{12(1-\nu^2)} \left(\frac{t}{h_B} \right)^2 \left(\frac{Y}{Y - h_A - h_{hole}} \right) \quad (15)$$

Where the final term in Eq. (15) converts the buckling stress from the edge of unstiffened strip “B” to the edge of unstiffened strip “A” so that the two stresses (f_{crA} and f_{crB}) may be compared in Eq. (12) to determine the minimum. The plate buckling coefficient for the unstiffened strip “B” is approximated as:

for $L_{hole}/h_B \geq 0.75$

$$k_B = 0.340\psi_B^2 + 0.100\psi_B + 0.573, \quad (16)$$

for $L_{hole}/h_B < 0.75$

$$k_B = 0.340\psi_B^2 + 0.100\psi_B + 0.573 + 15(0.75 - L_{hole}/h_B), \quad (17)$$

and the ratio of tension to compressive stresses is:

$$\psi_B = \frac{h - Y}{Y - h_A - h_{hole}}, \quad 0 \leq \psi_B \leq 10. \quad (18)$$

The plate buckling coefficient k_B is developed based on AISI-S100-07 Eq. B3.2-5 (AISI-S100 2007), but is modified to be applicable over a larger range of ψ_B and to account for the increase in k_B as the unstiffened strip aspect ratio tends to zero (i.e., a wide, short strip resulting from a small hole) (Moen 2008).

Conversion to the gross section for the comparison of stresses required in Eq. (9) requires that:

$$\text{for } h_A + h_{hole} \geq Y, \quad f_{crh} = f_{crh,net} \left(1 + \psi_A \right) \frac{h_A}{Y}, \quad (19)$$

$$\text{for } h_A + h_{hole} < Y, \quad f_{crh} = f_{crh,net} \left[1 - \frac{h_{hole}}{Y} \left(2\psi_A - \frac{h_{hole}}{Y} \right) \right]. \quad (20)$$

The conversion from $f_{crh,net}$ at the net section of the plate to f_{crh} on the gross cross-section is obtained with a similar method to that described in Figure 3 for stiffened elements in uniaxial compression; the total compressive force at the net and gross cross-sections are assumed in equilibrium (Moen 2008).

Unstiffened element in uniaxial compression

For an unstiffened element in compression with hole(s), the approximation considers buckling of the entire unstiffened element without holes, buckling of the entire unstiffened element with holes shown in Figure 5a, and buckling of the unstiffened strip adjacent to the hole at the simply-supported edge. The plate strip adjacent to the hole and the free edge exhibits Euler buckling as shown in Figure 5b as its aspect ratio increases, which is not predicted by this method, motivating the $L_{hole}/h_B \leq 10$ limit in Eq. (1).

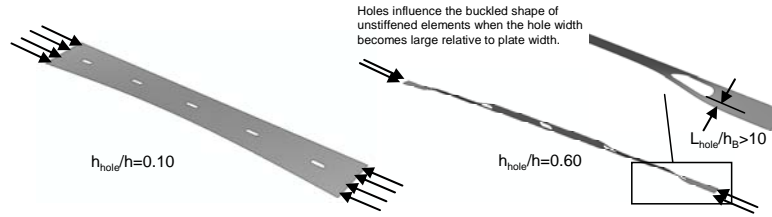


Figure 5 (a) Buckled mode shape of an unstiffened element with holes and (b) Euler buckling of the unstiffened strip at the free edge

The elastic buckling stress of an unstiffened element in compression with holes is thus approximated as:

$$f_{crl} = \min[f_{cr}, f_{crh}]. \quad (21)$$

The critical elastic buckling stress prediction for plate buckling of the unstiffened element without holes (f_{cr}) is calculated with Eq. (3), where $k=0.425$ when considering long rectangular plates ($L/h > 4$). The minimum critical elastic buckling stress of the unstiffened element with holes, f_{crh} , coincides with either buckling of the entire unstiffened element with holes or buckling of the unstiffened strip “A” adjacent to the hole and the simply supported edge, or:

$$f_{crh} = \min \left[k \frac{\pi^2 E}{12(1-\nu^2)} \left(\frac{t}{h} \right)^2, f_{crA} \left(1 - \frac{h_{hole}}{h} \right) \right] \quad (22)$$

where k is an empirical plate buckling coefficient derived from finite element eigenbuckling studies which reflect the reduced axial stiffness of an unstiffened element with holes (Moen 2008):

$$k = 0.425 \left(1 - 0.062 \frac{L_{hole}}{h_A} \right). \quad (23)$$

f_{crA} is calculated with Eq. (5) and modified by the factor $(1 - h_{hole}/h)$ to convert the stress on the unstiffened strip “A” to the stress at the end of the plate so that it can be compared to the buckling stress of the unstiffened element. f_{crh} will always be predicted as less than or equal to f_{cr} with this method.

Elastic buckling of members with holes

The element-based methods introduced in the previous section can be used as the first step for element-based effective width methods, or to approximate the (local) elastic buckling stress of cold-formed steel beams and columns. However, beam and column stability predictions determined from the element-based expressions are typically too conservative for use in DSM because they ignore beneficial inter-element interaction in the cross-section. Elastic buckling approximations are now presented for full cold-formed steel structural members with holes. The finite strip method is employed to predict local and distortional elastic buckling, and modifications to the classical column and beam stability equations are proposed for global buckling of cold-formed steel structural members with holes. Examples are presented which demonstrate the viability of the methods. Complete verification studies have also recently been completed and are provided in Moen (2008).

Local buckling

The approximate method for predicting the local elastic buckling behavior of cold-formed steel members with holes, presented here, is an extension of the element-based approximations, where local buckling is assumed to occur as either plate buckling of the entire cross-section or unstiffened strip buckling at the location of the hole. The use of the finite strip method allows for a more realistic prediction of P_{cr} (and M_{cr} in beams) including the interaction of the cross-section with the unstiffened strip.

The local critical elastic buckling load P_{cr} is approximated for a cold-formed steel column with holes as

$$P_{cr} = \min(P_{cr}, P_{crh}). \quad (24)$$

The calculation of the local critical elastic buckling load on the gross cross-section, P_{cr} is performed using standard procedures defined in Appendix 1 of AISI-S100-07 (AISI-S100 2007). P_{crh} is calculated with the finite strip software CUFSM (Schafer and Adany 2006) using the net cross-section shown in Figure 6. The corners of the cross-section are restrained in the z -direction in the finite strip model to isolate local buckling from distortional buckling of the cross

section. (This method of isolating local buckling is viable for C-section columns or beams with web holes. For other cross-section shapes and hole locations, fixity in the x -direction or both the x - and z -directions may be required.) An eigenbuckling analysis is performed with this net cross-section, and an elastic buckling curve is generated. The half-wavelength corresponding to the minimum buckling load is identified as L_{crh} . When $L_{hole} < L_{crh}$, as shown in Figure 6a, P_{crh} is equal to the buckling load at the length of the hole (FE and experimental studies support that buckling in the unstiffened strip occurs over the length of the hole). If $L_{hole} \geq L_{crh}$ as shown in Figure 6b, P_{crh} is obtained at the minimum on the buckling curve (as in this case the hole is long enough to allow the natural wavelength of the unstiffened strip to form). Determining elastic buckling loads at specific half-wavelengths is a new and fundamentally different use of the finite strip method when compared to its primary application within DSM, which is calculating the lowest fundamental elastic buckling modes of cold-formed steel members. This method can also be implemented in its current form to predict M_{crf} for beams with holes.

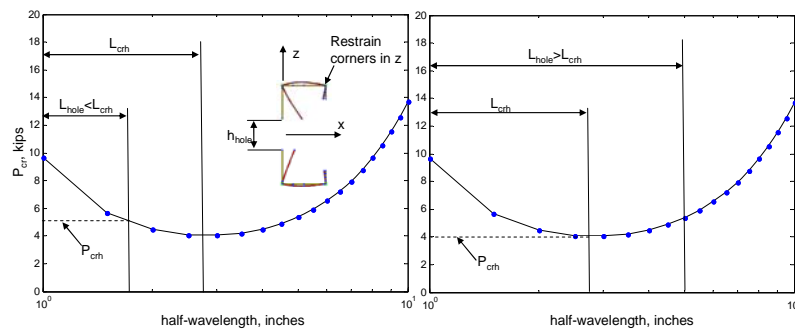


Figure 6 Local elastic buckling curve of net cross-section when (a) hole length is less than L_{crh} and (b) when hole length is greater than L_{crh}

An example is now presented where the approximate method is employed to calculate P_{crf} for a 100 in. (2540 mm) long column with an SSMA 362S162-33 cross section and evenly spaced slotted web holes where $S=20$ in. (508 mm) (SSMA 2001). Figure 7a compares the finite strip and ABAQUS mode shapes for $h_{hole}/h_C=0.14$, where h_C is the C-section web depth measured from the flange centerlines. The CUFSM approximate method predictions are plotted for a range of h_{hole}/h_C and compared with ABAQUS eigenbuckling predictions in Figure 7b. For this example, smaller hole widths lead to the largest reductions in P_{crf} . This counterintuitive result occurs because for small holes unstiffened strip buckling controls the local buckling behavior and for large holes, local buckling occurs between the holes. (One must keep in mind that for strength the net section in

yielding, as well as the elastic buckling load, ultimately determine the capacity, not just P_{crf} .)

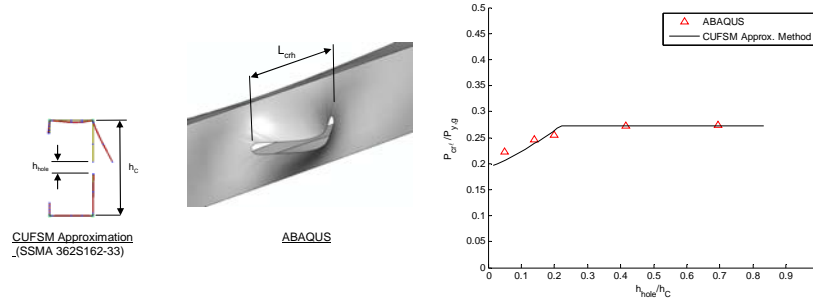


Figure 7 Comparison of CUFSM approximate method and ABAQUS local buckling (a) modes and (b) critical elastic buckling loads

Distortional buckling

An approximate method utilizing the finite strip method is introduced here for predicting the distortional critical elastic buckling load, P_{crdb} of cold-formed steel columns with holes. The method simulates the loss in bending stiffness of a C-section from the presence of a web hole within a distortional buckling half-wave by modifying the cross-section thickness in the finite strip method. The thickness of the entire web is reduced based on the relationship between web bending stiffness (derived with observations from ABAQUS thin shell elastic FE analyses) and the bending stiffness matrix terms of a finite strip element (Moen 2008). The distortional half-wavelength of the cross-section, L_{crdb} without holes is determined first using the gross section of the column in CUFSM to generate an elastic buckling curve. Half-wavelength L_{crd} is defined by the location of the distortional minimum, as shown in Figure 8. The web thickness is then modified in the finite strip method to account for the lost stiffness due to the holes via:

$$t_{web,hole} = \left(1 - \frac{L_{hole}}{L_{crd}}\right)^{1/3} t, \quad (25)$$

where t is the cross-section thickness. A similar modification to t has been proposed for web-slotted thermal structural studs (Kesti 2000). Finally, an additional finite strip analysis is performed and the elastic buckling curve is generated for the modified cross-section and P_{crd} (including the presence of the hole) is determined as the elastic buckling load occurring at L_{crd} as shown in Figure 8. Actually, only a single analysis at L_{crd} is required, but a range of L 's are shown in Figure 8 to illustrate the concept.

To demonstrate the method, the distortional critical elastic buckling load P_{crd} is approximated for a long column ($L=100$ in. or 2540 mm) with an SSMA 250S162-68 cross-section and five evenly spaced slotted web holes where $S=20$ in. (508 mm) and $L_{hole}=4$ in. (102 mm). The width of the hole is varied relative to the web width, and ABAQUS eigenbuckling results are used to evaluate the viability of the method. $P_{y,g}$ is the squash load of the column calculated with the gross cross-sectional area and assuming $F_y=50$ ksi (345 MPa). The ABAQUS distortional buckling mode shape is provided in Figure 8b, when $h_{hole}/h=0.63$. Nine distortional half-waves form along the member in ABAQUS, with every other half-wave containing one slotted hole. The CUFSM prediction method is compared over a range of h_{hole}/h to ABAQUS eigenbuckling results in Figure 8b, demonstrating that the CUFSM approximation is a viable predictor of P_{crd} . This approximate method has also been implemented successfully for C-section beams with web holes (Moen 2008).

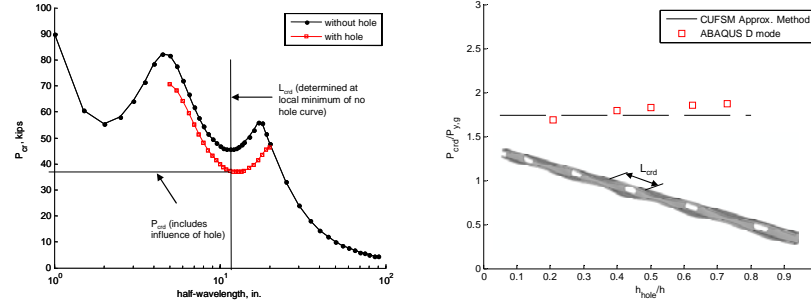


Figure 8 Distortional buckling (a) approximating P_{crd} for an SSMA 250S162-68 cross-section with holes and (b) comparing the approximate method to ABAQUS predictions

Global buckling

The exact solution for the global (flexural only) critical elastic buckling load P_{cre} of a column with holes symmetrically spaced about the longitudinal midline can be derived using energy methods based on classical expressions (Timoshenko 1961) modified to account for holes (Moen 2008):

$$P_{cre} = \frac{\pi^2 EI_{avg}}{L^2}, \quad (26)$$

where

$$I_{avg} = \left(\frac{I_g L_{NH} + I_{net} L_H}{L} \right). \quad (27)$$

I_g is the moment of inertia of the gross cross-section, I_{net} is the moment of inertia of the net cross-section, L_{NH} is the length of column without holes and L_H is the

length of column with holes (note that $L_{NH} + L_H = L$). I_{avg} is the weighted average of the gross and net cross section moment of inertia along the column length.

An approximate method for calculating P_{cre} is proposed here which extends this “weighted properties” methodology in Eq. (27) to all of the cross-section properties of the column required to solve the classical cubic buckling equation for columns (Chajes 1974):

$$\left(P_{cre,y} - P\right)\left(P_{cre,x} - P\right)\left(P_{cre,\phi} - P\right) - \left(P_{cre,y} - P\right)\frac{P^2 x_o^2}{r_o^2} - \left(P_{cre,x} - P\right)\frac{P^2 y_o^2}{r_o^2} = 0, \quad (28)$$

including the cross-sectional area A , moment of inertia I_x and I_y , St. Venant torsional constant J , and shear center location. The computer program CUTWP solves Eq. (28) for any general cross-section and is freely available (Sarawit 2006). The net section properties can be calculated in CUFSM (or CUTWP) by reducing the sheet strip thickness to zero at the location of the hole. The net section warping torsion constant $C_{w,net}$ is not as clearly defined though. If cross-section continuity at the hole is assumed, $C_{w,net}$ is calculated assuming the full cross-section is resistant to warping (i.e., the line integral used to solve for the warping function is continuous around the cross-section). This approach leads to unconservative (stiffer) predictions of the actual average C_w derived from thin shell FE analysis (Moen 2008). Research is ongoing in this area, but for now it is recommended to conservatively assume $C_{w,net}=0$ when calculating $C_{w,avg}$ for use in Eq. (28). In addition to the approximate method proposed here for evenly spaced holes along the member length, global buckling approximations for columns with a single hole or irregularly spaced holes have also been recently developed (Moen 2008).

ABAQUS global eigenbuckling results are compared to the “weighted properties” approximation for an SSMA 1200S162-68 long column with evenly spaced circular holes. The length of the column $L=100$ in. (2540 mm), the hole spacing $S=20$ in. (508 mm), and the diameter of the circular hole is varied from $h_{hole}/H=0.10$ to 0.90 where H is the out-to-out depth of the cross-section. Figure 9 provides the weak-axis flexural and flexural-torsional buckling modes when $h_{hole}/H=0.50$. Note that thin shell FE predicts local buckling mixing with the weak-axis flexural mode when $h_{hole}/H>0.50$ because P_{cre} is reduced by the presence of holes to a magnitude similar to the local critical elastic buckling load $P_{cr}=6.69$ kips (29.8 kN).

The gross cross-section properties A_g , $I_{x,g}$, $I_{y,g}$, $J_{y,g}$, $C_{w,g}$ and the gross centroid and shear center locations of the SSMA 1200S162-68 cross section are

calculated in CUFSM. The net section properties A_{net} , $I_{x,net}$, $I_{y,net}$, $J_{y,net}$, net centroid and shear center locations are then calculated in CUFSM assuming zero thickness at the hole. $C_{w,net}$ is conservatively assumed equal to zero. Eq. (27) is employed to obtain the average cross-section properties of the column, which are then used in the cubic column buckling equation of Eq. (28) (or equivalently CUTWP) to arrive at the approximate weak-axis flexural and flexural-torsional critical elastic buckling loads.

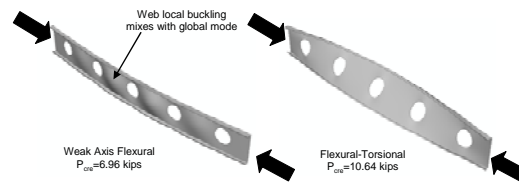


Figure 9 Weak-axis flexural and flexural-torsional global buckling modes for an SSMA 1200S162-68 column with evenly spaced circular holes

Figure 10a compares the weak-axis flexural critical elastic buckling load of the 1200S162-68 column calculated with the “weighted properties” prediction methods to ABAQUS eigenbuckling results. The ABAQUS calculation of P_{cre} is systematically 10% lower than the prediction method (even for a column without holes), which results from the assumption of a rigid cross-section in the classical stability equations. (The reduction in P_{cre} was confirmed in CUFSM, which like ABAQUS, accounts for plate-type deformations in elastic buckling calculations.) The approximate method is an accurate predictor of the weak-axis flexural P_{cre} , even when hole width becomes larger relative to web depth. The prediction of P_{cre} using just the net section properties is also plotted in Figure 10a as a conservative baseline.

Figure 10b compares the “weighted properties” methods to ABAQUS results for the second global mode, flexural-torsional column buckling. The accuracy of the prediction methods decrease with increase h_{hole}/H confirming that $C_{w,avg}$ calculated with $C_{w,net}$ assuming zero thickness at the hole, but otherwise continuous, overpredicts the average warping torsion stiffness of the column, especially as h_{hole}/H becomes large. Using $C_{w,net}=0$ in the “weighted properties” approach is shown to be a conservative predictor of P_{cre} , although work is ongoing to improve the accuracy of the method for modes involving torsional buckling. The “weighted properties” method can also be employed for predicting the global buckling of beams with evenly spaced holes (Moen 2008).

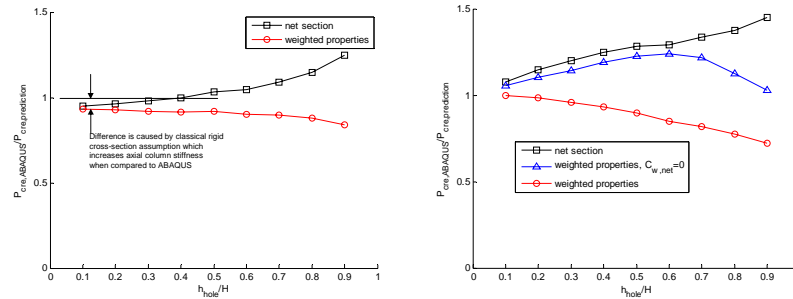


Figure 10 Comparison of “weighted properties” predictions to ABAQUS results for an SSMA 1200S162-68 column in (a) weak-axis flexural and (b) flexural-torsional buckling

Conclusions

Viable, conservative, approximate methods for predicting elastic buckling of cold-formed steel structural members with holes are presented here, both for elements and the entire member. The element-based approximations primarily rely on improvements to the unstiffened strip approach to account for hole length and stress gradients in the partially supported plates adjacent to the holes. Member-based approximations for local and distortional buckling of cold-formed steel rely on empirical modifications to the finite strip method to account for the new buckling modes introduced by the hole(s). For global buckling a “weighted properties” approach is proposed for cold-formed steel columns and beams with regularly spaced holes. Taken together the approximate methods provide a basic building block for needed improvements in both the element-based effective width method, and the member-based Direct Strength Method for the design of cold-formed steel structural members with holes.

Acknowledgements

This research was conducted under the generous sponsorship of the American Iron and Steel Institute (AISI) and reflects insightful contributions from the dedicated members of the AISI Committee on Specifications.

References

- AISI-S100. (2007). *North American Specification for the Design of Cold-Formed Steel Structural Members*, American Iron and Steel Institute, Washington, D.C.
- Brown, C.J., and Yettram, A.L. (2000). "Factors influencing the elastic stability of orthotropic plates containing a rectangular cut-out." *Journal of Strain Analysis for Engineering Design*, 35(6), 445-458.
- Chajes, A. (1974). *Principles of Structural Stability*, Prentice Hall College Div, Englewood Cliffs, NJ.
- El-Sawy, K.M., and Nazmy, A.S. (2001). "Effect of aspect ratio on the elastic buckling of uniaxially loaded plates with eccentric holes." *Thin-Walled Structures*, 39(12), 983-998.
- Kawai, T., and Ohtsubo, H. (1968). "A Method of Solution for the Complicated Buckling Problems of Elastic Plates with Combined Use of Rayleigh-Ritz's Procedure in the Finite Element Method." *Proceedings of the Second Conference on Matrix Methods in Structural Mechanics*, AFFDL-TR-68-150, Wright-Patterson Air Force Base, Ohio, 967-994.
- Kesti, J. (2000). "Local and Distortional Buckling of Perforated Steel Wall Studs," Dissertation/Thesis, Helsinki University of Technology, Espoo, Finland.
- Kumai, T. (1952). "Elastic stability of the square plate with a central circular hole under edge thrust." *Reports of Research Institute for Applied Mechanics*, 1(2).
- Miller, T.H., and Peköz, T. (1994). "Unstiffened strip approach for perforated wall studs." *ASCE Journal of Structural Engineering*, 120(2), 410-421.
- Moen, C.D. (2008). "Direct Strength Design for Cold-Formed Steel Members with Perforations," Ph.D. Thesis, Johns Hopkins University, Baltimore.
- Moen, C.D., and Schafer, B.W. (2006). "Impact of holes on the elastic buckling of cold-formed steel columns with applications to the Direct Strength Method." *Eighteenth International Specialty Conference on Cold-Formed Steel Structures*, Orlando, FL, 269-283.
- NAS. (2007). *Supplement to the North American Specification for the Design of Cold-Formed Steel Structural Members, Appendix 1*, American Iron and Steel Institute, Washington, D.C.
- Sarawit, A. (2003). "Cold-Formed Steel Frame and Beam-Column Design," Ph.D. Thesis, Cornell University, Ithaca.
- Sarawit, A. (2006). "CUTWP Thin-walled section properties, December 2006 update <www.ce.jhu.edu/bschafer/cutwp> ", accessed January 2008.
- Schafer, B.W. (2008). "Review: The Direct Strength Method of cold-formed steel member design." *Journal of Constructional Research*, 64(7/8), 766-778.
- Schafer, B.W., Adany, S. (2006). "Buckling analysis of cold-formed steel members using CUFSM: conventional and constrained finite strip methods." *Eighteenth International Specialty Conference on Cold-Formed Steel Structures*, Orlando, FL.
- Schlack Jr., A.L. (1964). "Elastic stability of pierced square plates." *Experimental Mechanics*, 4(6), 167-172.
- SSMA. (2001). "Product Technical Information, ICBO ER-4943P." Steel Stud Manufacturers Association, www.ssma.com.
- Timoshenko, S.P., Gere, James M. (1961). *Theory of Elastic Stability*, McGraw-Hill, New York.
- Tovar, J., and Sposito, T. (2005). "Application of direct strength method to axially loaded perforated cold-formed steel studs: Distortional and local buckling." *Thin-Walled Structures*, 43(12), 1882-1912.
- Vann, P.W. (1971). "Compressive buckling of perforated plate elements." *First Specialty Conference on Cold-formed Structures*, Rolla, Missouri, 58-64.
- Yoshiki, M., and Fujita, Y. (1967). "On the Buckling Strength of Perforated Plates (1)." *Proceedings of the Society of Naval Architects of Japan*, No. 122.
- Yu, C., and Schafer, B.W. (2007). "Effect of Longitudinal Stress Gradients on Elastic Buckling of Thin Plates." *ASCE Journal of Structural Engineering*, 133(4), 452-463.
- Yu, W.W., and Davis, C.S. (1973). "Cold-formed steel members with perforated elements." *ASCE J Struct Div*, 99(ST10), 2061-2077.

